Mitochondrially targeted redox probe reveals the variations in oxidative capacity of the haematopoietic cells

Journal:	*Organic & Biomolecular Chemistry*
Manuscript ID:	OB-COM-05-2015-000928.R1
Article Type:	Communication
Date Submitted by the Author:	18-May-2015

Complete List of Authors:	Kaur, Amandeep; University of Sydney, School of Chemistry Brigden, Kurt; University of Sydney, Discipline of Physiology, School of Medical Sciences; university of sydney, Cashman, Timothy; University of Sydney, School of Chemistry Fraser, Stuart; University of Sydney, Discipline of Physiology, School of Medical Sciences New, Elizabeth; University of Sydney, School of Chemistry

Journal Name

COMMUNICATION

Mitochondrially targeted redox probe reveals the variations in oxidative capacity of the haematopoietic cells

Received 00th January 20xx,
Accepted 00th January 20xx

DOI: 10.1039/x0xx00000x

www.rsc.org/

Amandeep Kaur,[a] Kurt W. L. Brigden,[b] Timothy F. Cashman,[a] Stuart T. Fraser,[b] Elizabeth J. New.[a]

Both oxidative stress and mitochondrial dysfunction play roles in a myriad of pathological conditions. There is therefore a need for tools that possess the ability to measure the dynamics of oxidative capacity within the mitochondria, particularly those that can measure reversible changes. Here, we report a mitochondrially-targeted fluorescent redox sensor NpFR2, which can reversibly measure changes in the mitochondrial redox environment. The probe has been used to report on variations in oxidative capacity of the haematopoietic cells in bone marrow, thymus and spleen.

Under normal conditions, cells tend to maintain a narrow window of cellular oxidative capacity by regulating the production and sequestration of reactive oxygen species (ROS).[1] Uncontrolled production of ROS leads to high cellular oxidative capacity, commonly termed "oxidative stress". Oxidative stress has long been linked to a range of pathological conditions, but recent studies indicate that the levels of cellular oxidative capacity depends not only on the cell type and function but also on the degree of maturation.[2–4] Elucidating the role of this cellular oxidative capacity in physiology and pathology is of great current interest.

The mitochondrion - the cell's power house - plays a key role in the regulation of redox homeostasis. Along with the electron transport chain (ETC), which is the site for ATP production and the generation of ROS, this organelle also houses various membrane-bound redox regulatory proteins.[5] Some studies suggest that mitochondria dictate cellular fate, whether maturation or apoptosis, by appropriate manipulation of the cell's redox homeostasis.[6–8] A thorough understanding of the mitochondrial redox state will therefore give an insight into its physiological functions.

Whilst mitochondrial ROS are clearly associated with disease states, they hves also been implicated in regulating homeostatic cellular physiology. Processes such as responding to hypoxia, immune responses, cellular differentiation and maturation, as well as autophagy and ageing, have all been linked to mitochondrial ROS levels. The cells of the haematopoietic (blood) lineage are formed in the adult bone marrow, engage in immune responses against pathogens, proceed through highly orchestrated differentiation pathways and exhibit unique metabolic processes.[9,10] We have therefore used the haematopoietic lineages as a model system for studying mitochondrial ROS.

In order to elucidate the role of mitochondrial redox state, we require a fluorescent redox probe that is reversible, with a reduction potential within the biologically relevant range. To date, several fluorescent mitochondrial probes have been designed based on small organic molecules, the majority of which are reaction-based, and hence irreversible.[11–13] Amongst the small number of reversible redox probes, most are cytoplasmic.[14–18] We have previously reported a reversible fluorescent redox probe that was able to report on the cytoplasmic redox state.[19] We have suitably modified this probe to localise within the mitochondria without affecting its fluorescence properties or redox potential. A well-established method of targeting molecules to the mitochondria involves incorporation of a triphenyl phosphonium (TPP) group into the molecule.[20,21] The negatively charged mitochondrial membrane preferentially localises the positively-charged TPP moiety. We report here a novel mitochondrial targeted reversible redox probe naphthalimide – flavin redox sensor 2 (**NpFR2**) (Figure 1a) and its application in the study of murine haematopoietic cells within the bone marrow, thymus and spleen.

The design of **NpFR2** is based on a modified flavin molecule, with incorporation of a triphenylphosphonium (TPP) moiety at the end of an aliphatic side chain at *N*-8 position. **NpFR2** was synthesised by the alloxan monohydrate method[22] (Scheme S1). The TPP salt of 3-aminopropylbromide was used to alkylate 4-bromo-1,8-napthalic anhydride to give 4-bromo-*N*-(3-triphenylphosphonium propyl)-1,8-naphthalimide, followed by nitration, to afford the corresponding 3-nitro derivative. Alkylation with propylamine gave the 4-propylamino compound that was then reduced to give the *O*-diamino naphthalimide derivative, which on reaction with alloxan monohydrate in the presence of boric acid afforded **NpFR2**.

[a] School of Chemistry, The University of Sydney, New South Wales 2006, Australia.
[b] Discipline of Physiology, School of Medical Sciences, The University of Sydney, New South Wales 2006, Australia.

† Footnotes relating to the title and/or authors should appear here.
Electronic Supplementary Information (ESI) available: [details of any supplementary information available should be included here]. See DOI: 10.1039/x0xx00000x

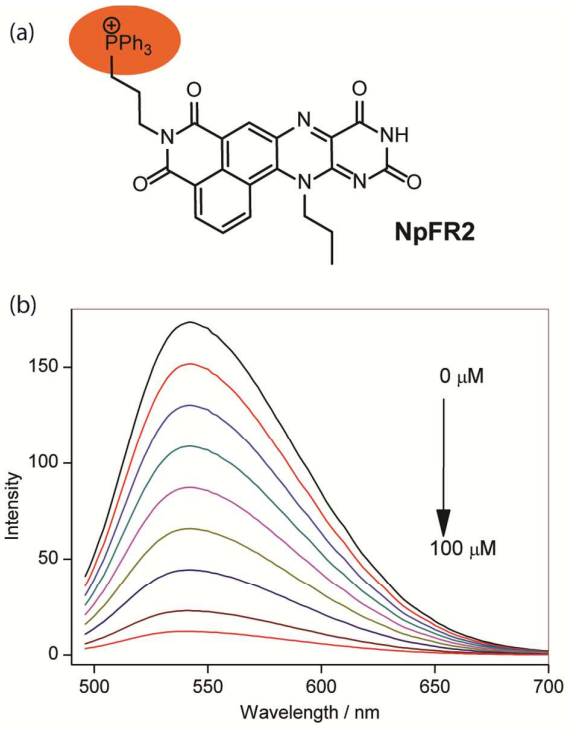

Figure 1. (a) Chemical structure of **NpFR2** showing TPP – mitochondrial targeting moiety. (b) Fluorescence emission of **NpFR2** (10 μM, λ_{ex} = 488 nm) with the incremental addition of sodium dithionite.

Photophysical properties of **NpFR2** were tested in HEPES buffer (100 mM, pH 7.4). As expected, the photophysical behaviour of **NpFR2** was similar to that of the previously-reported, flavin-containing redox probe, **NpFR1**.[19] In the oxidised form, **NpFR2** is a planar molecule with a maximum absorption at 470, 489 and 530 nm (log ε = 3.8, 5.9 and 3.1 respectively), and maximum emission at 545 nm (Φ = 0.26) (Figure S1). Reduction of **NpFR2** could be achieved with a range of mild reducing agents such as sodium dithionite, sodium cyanoborohydride, glutathione (GSH) and dithiothreitol (DTT). The reduced form of the probe exhibits 115-fold lower emission, consistent with bending of the molecule (Figure 1b). Furthermore, the reduced form of **NpFR2** could be re-oxidised by hydrogen peroxide restoring its original absorbance and fluorescence profiles. This reduction-oxidation cycle could be repeated for up to 7 cycles without significant loss in fluorescence response (Figure S2), thus highlighting the reversible redox-responsive properties of **NpFR2**. Re-oxidation of **NpFR2** is rapid, with 95% of the original fluorescence restored within 5 minutes of H_2O_2 addition (Figure S3). The fluorescence properties of **NpFR2** as well as the kinetics of re-oxidation suggest that **NpFR2** follows a similar sensing mechanism to that of riboflavin and **NpFR1**,[19,23] confirming that the TPP tag has not affected these properties. In addition, re-oxidation of **NpFR2** could be achieved by a range of diverse oxidants (Figure S4), demonstrating that **NpFR2** can be used as a sensor for the global redox state rather than a single ROS. Control experiments confirm that the emission profiles of **NpFR2** in the oxidised or reduced form are unaffected by the presence of biologically relevant metal ions (Figure S5) and remain constant over the pH range 2-9 (Figure S6). **NpFR2** can therefore be utilised in physiological conditions without any background interference.

After establishing the redox-responsive properties and reversibility of **NpFR2**, we sought to test its subcellular localisation in cultured cells, using murine macrophages (RAW 264.7 cells) and ovarian carcinoma (HeLa) cells. Under excitation by a 488 laser, control cells untreated with the probe showed negligible fluorescence, while cells treated with **NpFR2** (20 μM, 15 min) showed significant fluorescence. Cells were co-stained with **NpFR2** (10 μM, 15 min) and the commercially-available Mitotracker DeepRed FM (100 nM, 15 min) and fluorescence images obtained in green and red channels respectively. For both RAW 264.7 and HeLa cells, the fluorescence of **NpFR2** from the co-stained cell overlaps well with that of the mitotracker as indicated by the yellow regions in the merged image (Figures 2(a), S7 and S8), and the high Pearson's co-localisation coefficients (0.94 and 0.92 respectively) obtained from the intensity correlation plots (Figures S7(e4) and S8(d4)). Furthermore, co-staining of RAW 264.7 cells with **NpFR2** and Lysotracker DeepRed revealed significantly different localisation profiles regions, accompanied by a poor Pearson's co-localisation coefficient of 0.10 (Figure S7(f4)). Finally, images obtained from cells singly-stained with **NpFR2**, Mitotracker or Lysotracker confirmed that no emission leaked from one channel into the other (Figure S7(b), (c) and (d)). The cytotoxicity of **NpFR2** in HeLa cells was determined by MTT assay, and revealed an IC_{50} value of 65 μM for 24 h – far above the incubation time and concentrations used in all cellular experiments.

Having observed the mitochondrial localisation of **NpFR2** in cultured cells by microscopy, we assessed whether this probe could be used for live, single cell analysis by flow cytometry in specific haematopoietic cell types. Single cell suspensions of bone marrow, thymus and spleen samples were incubated with

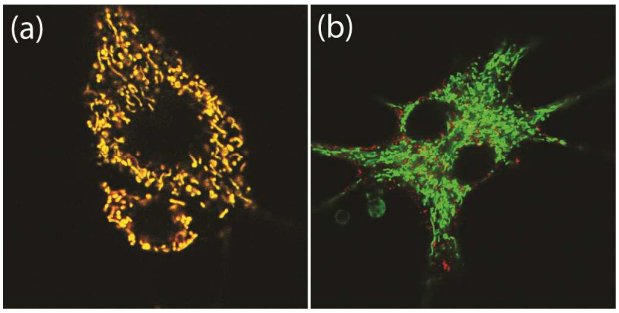

Figure 2. Co-localisation images of macrophages (RAW 264.7) treated with **NpFR2** (20 μM, λ_{ex} = 488 nm, λ_{em} = 495-600 nm) and (a) Mitotracker deep red (100 nM, λ_{ex} = 633 nm, λ_{em} = 650-750 nm) and (b) Lysotracker deep red (100 nM, λ_{ex} = 633 nm, λ_{em} = 650-750 nm) for 15 mins. Yellow regions indicate co-localisation.

NpFR2 and then assessed for fluorescence using a flow cytometer. **NpFR2** fluorescence could be detected in fluorescent channels 1 (488 nm excitation, 530/30 nm emission) and 2 (488 nm excitation, 585/42 nm emission) of the BD FACScan flow cytometer. Bone marrow cells showed a range of **NpFR2** fluorescent signals from negative to very bright (Figure 3a). In order to identify the populations to which these cells belonged, bone marrow cells were incubated with various antibodies. The

anti-CD45 antibody conjugated to allophycocyanin, which has red fluorescence emission, was used to identify maturing erythroid or red blood cells, which are the only haematopoietic cell types that do not express the CD45 antigen. Erythroid (forming red blood cells) cells were identified by use of the lineage-specific molecule Ter-119. We could detect two distinct populations, one with Ter-119 expression and high levels of **NpFR2** fluorescence, representing developing erythroid cells and a second with Ter-119 expression but no **NpFR2** fluorescence. This second population corresponds with the phenotype of mature erythrocytes, which express Ter-119 but lack mitochondria (Figure 3c). Macrophages can be identified by expression of F4/80 on their surface and showed two forms of **NpFR2**, suggesting bone marrow macrophages have high or low levels of mitochondrial ROS.

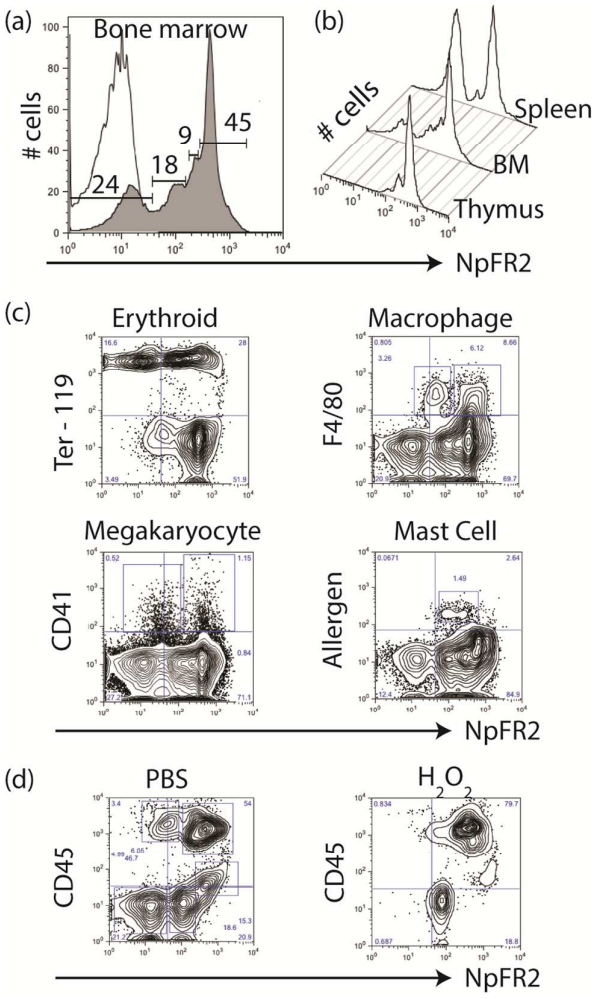

Figure 3. Detection of mitochondrial ROS species in haematopoietic cell types using **NpFR2** (20 µM, 15 min) by flow cytometry. (a) Bone marrow single cells were incubated with **NpFR2** (tinted profile) compared to unstained cells (unfilled profile). Numbers indicate frequency of total live, gated events. (b) Offset fluorescence of **NpFR2** fluorescent signal in thymus, bone marrow (BM) and spleen single cell suspensions. (c) **NpFR2** fluorescence in CD45-labelled haematopoietic cells after treatment with vehicle control (PBS) and H_2O_2. (d) **NpFR2** fluorescence in various bone marrow-derived haematopoietic cell types: Ter-119 positive (erythroid cells); F4/80-expressing (macrophages); CD41-expressing (megakaryocytes) and allergen-expressing (mast cells).

A similar pattern of **NpFR2** fluorescence was observed in CD41-expressing megakaryocytes (which form platelets), whilst mast cells (marked by expression of allergen) showed relatively uniform **NpFR2** fluorescence. Furthermore, treatment with hydrogen peroxide was found to increase **NpFR2** fluorescence in all bone marrow cells, regardless of CD45 expression level (Figure 3d). We also assessed **NpFR2** in the same lineage of cells in different haematopoietic organs; the bone marrow (site of most haematopoietic cell production), thymus (site of T lymphocyte maturation) and the spleen (site of immune cell function and destruction of aged and damaged red blood cells) (Figures 3 and 4). The bone marrow showed a range of **NpFR2** fluorescence, the thymus showed only one **NpFR2**-bright peak and a smaller **NpFR2**-medium peak. The spleen contained cells showing very low **NpFR2** fluorescence and a second peak of **NpFR2** - bright cells (Figure 3b).

CD4-expressing T lymphocytes arise from rare progenitors in the bone marrow and showed low/negative **NpFR2** fluorescence (Figure 4a). The thymus is the primary site of CD4-positive cell expansion and education. **NpFR2** is present in the vast majority of these cells, reflecting their highly proliferative state. In the spleen, mature functional CD4-positive T helper lymphocytes respond to immune challenges. This may be reflected by their high **NpFR2**-fluorescence. We also observed a small population (~1%) of CD4-positive cells lacking **NpFR2** fluorescence. These may correspond to memory CD4 T helper lymphocytes which reside in the spleen following exposure to pathogens in a highly quiescent state. Finally, to confirm that changes we were observing in **NpFR2** fluorescence were due to changes in mitochondrial redox rather than mitochondrial number, we coincubated with **NpFR2** and Mitotracker Deep Red. Bone marrow cells can be grouped into two cell types: Mitotracker Deep Red-negative, **NpFR2**-negative (which most likely represent mature erythrocytes lacking mitochondria), and Mitotracker Deep Red, **NpFR2**- double positive cells showing fluorescence from both mitochondrial probes. Most

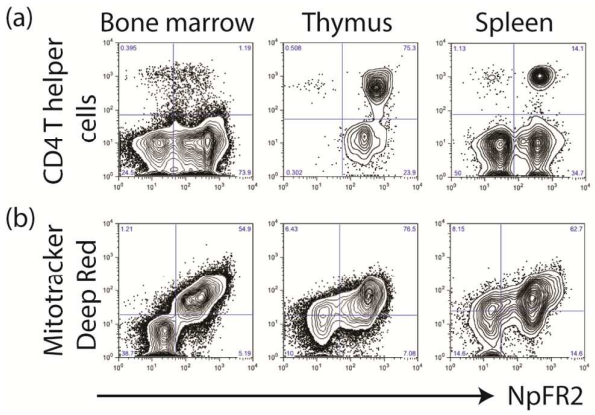

Figure 4. (a) **NpFR2** fluorescence in CD4-expressing T helper lymphocytes from different organs. Mitochondrial ROS as detected by **NpFR2** varies according to the site the CD4-expressing cell is found. (b) Comparison of mitochondrial number (Mitotracker) and mitochondrial ROS (**NpFR2**) in different haematopoietic organs. Data shows representative flow cytometric profiles from at least three independent experiments.

cells in the thymus showed fluorescence from both dyes. A similar situation occurred in the spleen samples, but we could also

detect a population which showed Mitotracker Deep Red fluorescence in the absence of **NpFR2** fluorescence indicative of a cell type with mitochondria that did not contain ROS (Figure 4b). This confirms that **NpFR2** can provide unique information about mitochondrial redox state. In summary, **NpFR2** is an excellent probe for detecting the varying levels of mitochondrial ROS and can be combined with other fluorescent probes and antibodies to dissect the role of mitochondrial ROS in different blood cells during development, maturation, proliferation and function.

Notes and references

1 H. Sies, *Exp Physiol*, 1997, **82**, 291–295.
2 M. Valko, D. Leibfritz, J. Moncol, M. T. Cronin, M. Mazur and J. Telser, *Int J Biochem Cell Biol*, 2007, **39**, 44–84.
3 E. H. Sarsour, M. G. Kumar, L. Chaudhuri, A. L. Kalen and P. C. Goswami, *Antioxid Redox Signal*, 2009, **11**, 2985–3011.
4 Y. M. Go and D. P. Jones, *Biochim Biophys Acta*, 2008, **1780**, 1273–1290.
5 M. P. Murphy, *Biochem. J.*, 2009, **417**, 1–13.
6 A. A. Starkov, *Ann N Y Acad Sci*, 2008, **1147**, 37–52.
7 K. Sinha, J. Das, P. B. Pal and P. C. Sil, *Arch Toxicol*, 2013, **87**, 1157–1180.
8 M. D. Brand, C. Affourtit, T. C. Esteves, K. Green, A. J. Lambert, S. Miwa, J. L. Pakay and N. Parker, *Free Radic Biol Med*, 2004, **37**, 755–767.
9 S. Ghaffari, *Antioxid. Redox Signal.*, 2008, **10**, 1923–1940.
10 N. Urao and M. Ushio-Fukai, *Free Radic. Biol. Med.*, 2013, **54**, 26–39.
11 Y. Koide, Y. Urano, S. Kenmoku, H. Kojima and T. Nagano, *J. Am. Chem. Soc.*, 2007, **129**, 10324–10325.
12 B. C. Dickinson and C. J. Chang, *J. Am. Chem. Soc.*, 2008, **130**, 9638–9639.
13 A. M. James, H. M. Cochemé and M. P. Murphy, *Mech. Ageing Dev.*, 2005, **126**, 982–986.
14 K. Xu, M. Qiang, W. Gao, R. Su, N. Li, Y. Gao, Y. Xie, F. Kong and B. Tang, *Chem. Sci.*, 2013, **4**, 1079–1086.
15 Y. Koide, M. Kawaguchi, Y. Urano, K. Hanaoka, T. Komatsu, M. Abo, T. Terai and T. Nagano, *Chem. Commun.*, 2012, **48**, 3091–3093.
16 E. W. Miller and C. J. Chang, *Curr. Opin. Chem. Biol.*, 2007, **11**, 620–625.
17 B. Wang, P. Li, F. Yu, J. Chen, Z. Qu and K. Han, *Chem. Commun.*, 2013, **49**, 5790–5792.
18 F. Yu, P. Li, B. Wang and K. Han, *J. Am. Chem. Soc.*, 2013, **135**, 7674–7680.
19 J. Yeow, A. Kaur, M. D. Anscomb and E. J. New, *Chem. Commun.*, 2014, **50**, 8181–8184.
20 M. P. Murphy, *Drug-Induced Mitochondrial Dysfunct.*, 2008, 575–587.
21 M. F. Ross, T. A. Prime, I. Abakumova, A. M. James, C. M. Porteous, R. A. J. Smith and M. P. Murphy, *Biochem. J.*, 2008, **411**, 633–645.
22 R. Kuhn and K. Reinemund, *Berichte der Dtsch. Chem. Gesellschaft (A B Ser.*, 1934, **67**, 1932–1936.
23 V. Favaudon, *Eur. J. Biochem.*, 1977, **78**, 293–307.